CFD Simulation in Predicting Slurry Flow in Horizontal Pipe

By

AIDIL YUNUS BIN ISMAIL
16760

Dissertation submitted in partial fulfilment of

the requirements for the

Bachelor of Engineering (Hons)

(Petroleum)

MAY 2015

Supervisor
MR. TITUS NTOW OFEI

Universiti Teknologi PETRONAS
Bandar Seri Iskandar
31750 Tronoh
Perak Darul Ridzuan

CERTIFICATION OF APPROVAL

CFD Simulation in Predicting Slurry Flow in Pipe

by

Aidil Yunus Bin Ismail

16760

A project dissertation submitted to the

Petroleum Engineering Programme

Universiti Teknologi PETRONAS

In partial fulfilment of the requirements for the

Degree of Engineering (Hons)

(Petroleum)

.

Approved by,

.....

(Mr. Titus Ntow Ofei)

Approved by,

……

(Mr.Asif Zamir)

UNIVERSITI TEKNOLOGI PETRONAS

TRONOH, PERAK

MAY 2015

CERTIFICATION OF ORIGINALITY

This is to certify that I am responsible for the work submitted in this project, that the original work is my own except as specified in the references and acknowledgements, and that the original work contained herein have not been undertaken or done by unspecified sources or persons.

.....

(Aidil Yunus Bin Ismail)

ABSTRACT

Slurry is the combination of two elements, solid-liquid mixtures. Pipe flows of slurry are commonly used in many applications of engineering fields for example pharmaceutical, food, civil, oil and gas and many other industries. Concern arises when the rate of transporting slurry plays an important role for the operation execution, especially regarding efficiency of operation, time management and maintenance cost. Its vital contribution to all sectors makes researchers believe that by developing the accurate model (simulation) can lead to an efficient reference during designing phase. Perhaps it can gives better diameter selection of slurry pipe, pumps selection and better power consumption which can economically help investors and developers. Studies have proven that there are many factors that can influence slurry behavior in pipeline. These factors include fluid types, size of the particles, mixtures velocities, solid volume fraction, pressure loss across the pipe and etc. This project focuses to comprehend the effect of particle size and solid volume fraction on solid concentration profile, cuttings velocity, and frictional pressure loss in horizontal pipeline. The Eulerian-Eulerian two-fluid model was adopted to simulate solid-water slurry flow in horizontal pipe. The model geometry and meshing were designed using ANSYS Workbench, while the flow equations were solved using ANSYS CFX 15.0 solver. The model compared satisfactorily with experimental cuttings concentration data in literature, thus confirming the validity of the current model setup. The k-ε turbulence model proved more robust than other turbulence models in comparison to the experimental results. Results from this study show that cuttings tend to accumulate at the end of the pipe as particles lose their momentum due to gravity at various particle size and cutting volume fraction. Furthermore, increasing the cutting volume fraction resulted in increase of pressure loss for all particle size, however, larger particle sizes resulted in lower pressure loss due to lower friction between particle and particle, particle to fluid and particle to wall. Finally, particle settling becomes more pronounced for larger particle sizes, leading to higher particle concentrations near the bottom of the pipe. The study shows how CFD analysis can replicate the actual transport operation, thus providing a better predictive model for engineers.

Acknowledgement

I would to express my deepest gratitude and appreciation to my supervisor, Mr. Titus Ntow Ofei who in spite of being extraordinarily busy with his duties, took time out to listen, to guide, to discuss and to follow though my final year project. He really helped me in understanding my final year project in a better perspective.

I wish to express my indebted gratitude to Universiti Teknologi PETRONAS (UTP) for the opportunity to study in this esteemed university and to allow me to conduct my entire experiments in UTP.

Besides, I would to like to acknowledge all ANSYS Lab technicians in Block 15 for their support and guidance in this project.

Besides, I would to give my sincere gratitude to my family, relatives, friends and lecturers of Geosciences and Petroleum Engineering for their support and assistance in this project.

Thank you.

Table of Contents

CHAPTER 1 INTRODUCTION 1
1.1 Project Background 1
1.2 Problem Statement 2
1.3 Objective: 2
1.4 Scope of study: 2
CHAPTER 2 LITERATURE REVIEW 3
2.1.1 One layer model 3
2.1.2 Two layer model 4
2.1.3 Three layer model 4
2.2 Effect of Particle size on Pressure loss 4
2.3 Effect of solid volume fraction and mixture velocity on concentration profile . 6
CHAPTER 3 METHODOLOGY 7
2.2 Research Methodology 7
2.3 Mathematical Modelling 7
2.3.1 Continuity equation 7
2.3.2 Momentum equation 8
2.3.3 Closure model 9
3.3 Geometry Modelling 10
3.4 Meshing and Grid independence study 10
3.5 Boundary Condition 12
3.6 Parametric study 12
3.7 Benchmarking: CFX Model Validation with Experimental Data 13
3.7.1 The RNG k-epsilon Model in ANSYS CFX 14
3.7.2 The k-omega Model 14
3.7.3 The SSG Reynold Stress 15
3.7.4 The Shear Stress Transport 16
3.7.5 Eddy Viscosity Transport 16
3.8 Design of Experiment 17
3.9 Key Milestone 19
3.9.1 Gantt Chart 20
CHAPTER 4 RESULT AND DISCUSSION 21

4.1 Benchmarking Study Result 21
4.2 Cutting Volume Fraction 22
4.3Effect of Particle size on Pressure loss at various cutting concentration 23
4.4 Effect of Particle size on Radial particle concentration profile 25
4.5Effect of particle size and concentration on cuttings velocity 26
CHAPTER 5 CONCLUSION AND RECOMMENDATION 27
REFERENCE 28
APPENDIXES 31

LIST OF FIGURES

Figure 1: Effect of solid particle size on the slurry pressure loss at Cv= 5% [7] 5
Figure 2: Effect of solid particle size on the slurry pressure loss at C_V= 25% [7] 5
Figure 3: Pressure loss against Element size. 11
Figure 4 : Meshing 3-dimensional view 12
Figure 5: Benchmarking Graph 21
Figure 6: Cutting volume fraction at outlet with variation particle sizes and cutting concentration at mixture's velocity of 5.4 m/s 22
Figure 7: Effect of Particle size on Pressure loss at various cutting concentration. 23
Figure 8: Effect of Particle size on Radial particle concentration profile at different cuttings concentration (10%, 25% and 40%). 25
Figure 9: Effect of particle size and concentration on cutting velocity 26
Figure 10: Cutting volume fraction at outlet with variation particle sizes and cutting concentration at mixture's velocity of 5.4 m/s (side view) 31

LIST OF TABLES

Table 1: Geometry modeling 10
Table 2 : Meshing and Grid Independence information 11
Table 3 : Experimental Data by [10] used as Benchmarking Validation 13
Table 4: Design of Experiment 18
Table 5: Experimental parameters [10] 19
Table 6: Key milestone 19
Table 7: Gantt chart 20

CHAPTER 1
INTRODUCTION

1.1 Project Background

Conveyance of slurries through pipelines is common throughout all over the worlds. Over decades, world constantly flows their slurries through pipelines for food industries, pharmaceutical, solid handling, tailing, and even power generation. Its vital contribution to all sectors makes researchers believe that by developing the accurate model (simulation) can lead to an efficient reference during designing phase. Perhaps it can gives better diameter selection of slurry pipe, pumps selection and better power consumption which can economically help investors and developers.

There are many factors that can affect the slurries flow behavior in pipelines for instance particle size, velocity profile, pressure loss, and concentration profile [1-4]. Past studies suggest many empirical correlations to predict fluid's behavior; however their capability is limited to some data range and experimental set up.

In oil and gas industry, applications of horizontal well has increased especially in cementing operations and hydraulic fracturing treatment. To have an efficient design on both, accurate prediction on the transport slurry properties in horizontal pipe is required.

Recently, Computational Fluid Dynamic (CFD) becomes an ultimate tool for predicting in the area like fluid movement behavior as it has the capability to tackle unlimited number of physical and operation conditions [5]. By developing mathematical equation and solve using a numerical algorithm on a computer, it is possible to control and extend the application of CFD models [2].

Last but not least, CFD software enable to provide more rapid result as well as more cases circumstances, make it a cost-effective tools to be use [6].

1.2 Problem Statement

Inaccurate information regarding particles size distribution, cutting volume fractions and mixture velocity often cause long distance transporting problems, high pressure losses and excessive erosion during cementing operation and hydraulic fracturing process.

Despite significant research work, empirical correlations obtained from experimental data contributed to the design of slurry pipelines [4]. By having a very limited database, correlation is prone to multiply its uncertainties and consequently will affect the final product [7]. To add, there are still lacks of experimental data on small variation of concentration available due to difficulties in measurement technique. As noted, existing models tends to provides macroscopic parameters for narrowly sized slurry only while industries of this world demanding variation of particle sizes [8, 9].

1.3 Objective:

The main objectives of this project are:

1. To simulate flow of slurry in pipeline using CFD
2. To predict the effect of particle size and solid volume fraction on solid concentration profile, cutting velocity and frictional pressure loss in pipeline.

1.4 Scope of study:

The scope of this project is bound to predicting slurry flow in pipeline, assuming fully developed fluid flow and steady state condition. Developing this model will employ Computational Fluid Dynamics (CFD) ANSYS-CFX.

Those techniques will cover the following aspects:

1. Design a simulation flow of slurry model in pipeline using ANSYS, which validated with experimental results.
2. Study the effect of particle size and solid volume fraction on solid concentration profile, cutting velocity and frictional pressure loss in pipeline.

CHAPTER 2
LITERATURE REVIEW

As mentioned earlier, a lot of work had been done to study and predict the slurry flow in pipelines especially regarding the information relates to velocity profile, concentration profile, pressure loss and particle size effect. According to [4,7] simulation result shows an affirmative with the published experimental data by gornvening Euler-Euler correlation along the standard k-Ɛ turbulence with mixture properties model.

Previous effort shows that because of gravitional effect slurry particles distributed asymmetrically in the vertical plane, and the degree of asymmetry increasing with the increase in particle size [2]. In addition, asymmetry reduces as concentration increase due to the disturbance effect between the solid particles at given velocity [9].

2.1.1 One layer model

An approach related to slurry flow modelling started where one-dimensional Schmidt-Rouse equation [10] (or equivalent to Hunt [11]) was developed to relate the particle sedimentation rate to the turbulence exchange rate, as represented by solid eddy diffusivity. Based on this formulation Karabelas [12] built an empirical model to predict the profile of particle concentration, work done by him then continued by Kausal and co-workers [13-17] to develope a diffusion model. The model proposed a modification for solid diffusivity for course slurry flow and their function shows that increasing solid concentration is due to increasing in the solid diffusivity. However it was done without taking solid diffusivity on both size and pipe Reynold number [18] into consideration. By comparing their pressure loss data with modified Wasp model they found match at higher fluid velocity, however significant deviation shows at flow velocities near the depositon velocity [19].

2.1.2 Two layer model

One dimensional two-layer model considering coarse-particle slurry was developed by Wilson [20] compromising two separate layers. He takes each layer a uniform velocity and concentration because he assume particles were very coarse. Doron at al.[21] developed model (two dimensional) to predict flow patterns and pressure loss which similar to Wilson [20], which also assumed lower layer as stationary. Wilson and Pough [22] expand dispersive force model by accounted particles suspended by fluid turbulence and contact-load (Columbic) friction, as result they find a good agreement with experimental in predicting particles concentration and velocity profile.

2.1.3 Three layer model

Doron and Barnea [23] extend to a three-layer model of slurry fluid flow in horizontal pipeline which consist of suspended layer, bed layer and dispersive layer (layer lies in between suspended and bed). They assume dispersive layer to be high in concentration gradient and the suspended layer, and no slip condition between fluid and solid particles. The model prediction successfully showed an assent with experimental data. Ramadan et al. [24] also extend to three dimensional-layer. Model prediction were then compared with the experimental, which clearly shows that there still a room of improvement can be done.

2.2 Effect of Particle size on Pressure loss

Figure 1 and Figure 2 [7] showing how solid particle size behaves accordingly. It is comparing the pressure gradient of different particles size at constant velocity and volume fraction range. By observing to this figures, finer particles prone to have less pressure loss (at all concentration and velocities) than medium and coarser particles [10]. At high concentration and low velocity coarser particle shows an increment of pressure loss, this is due to the accumulation of particles moving in pipeline's bed pulled by gravitational forces. While pressure loss in the finer particles, it increase the surface area in the suspension consequently

contribute to higher frictional losses. As the slurry velocity increase, the pressure loss's different of different particles becoming decreased. In figure 2, high solid concentration (25%) showing greatest pressure loss slope from fine slurry particles, therefore at 5m/s (high velocity) pressure loss of fine particles greater than medium size of slurry.

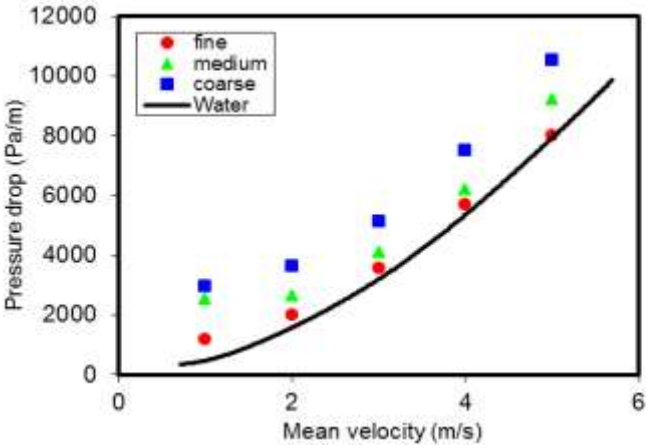

Figure 1: Effect of solid particle size on the slurry pressure loss at Cv= 5% [7]

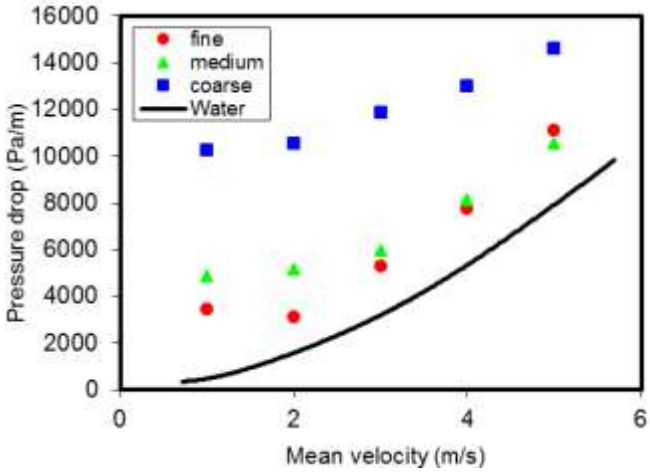

Figure 2: Effect of solid particle size on the slurry pressure loss at C_V= 25% [7]

2.3 Effect of solid volume fraction and mixture velocity on concentration profile

Data represented by [7] will assist in understanding the effect of volume fraction and mixture velocity on concentration profile. It shows concentration profile at various solid (sand) volume fraction, mixture velocities and particles sizes. The particles asymmetry behaving depends on particles size. The degree of asymmetry is directly proportional to the particles size due to the gravitational effect. While it is observed that the degree of asymmetry is inversely proportional to the mixture velocity at constant volume fraction [7].

From these [7] it also tell us that increasing interference effect in between solid particles makes increasing concentration lowers the asymmetry at given velocity. Therefore it can be conclude that degree asymmetry in concentration profile depends on particles size, solid volume fraction and mixture velocity [17].

CHAPTER 3
METHODOLOGY

2.2 Research Methodology

Methodology is a series of processes undergrowth during realizing objectives of the project. Simulation used in order to realize the project‘s objective is Computational Fluid Dynamic which govern Euler-Euler correlation along with the standard k-Ɛ turbulence with mixture properties model [4,7].

2.3 Mathematical Modelling

Model builds in this CFD based on the extended two-fluid model, which implement granular kinetic theory to describe interaction of particles. Particles are assumed to be spherical, inelastic, and flows with binary collision. Each phase is then solved by the fundamental of equation of momentum, mass and conservation of energy.

To close the conservation equations, suitable equation has to be selected in order to describe the rheological and/or physical properties for each phase. For this time, several equations and theories had been adopted to fulfill the agreement between simulation and experimental results’ requirement as instance: Continuity and Momentum Equation, Kinetic Theory of Granular Flow, Interfacial Force (momentum), Turbulence Equations and last but not least the Boundary Condition applied to the simulation model.

2.3.1 Continuity equation

Two phase conservation equations obtained by performing energy, mass and momentum balances on independent phase. Continuity equation descibes as the rate of mass entering the system equivalent to the mass leaving, assuming isothermal flow condition. liquid phase;

$$\frac{\partial \rho_l}{\partial t} + V.(\rho_l v_l) = 0 \qquad (1)$$

Solid Phase equation:

$$\frac{\partial \rho_s}{\partial t} + V.(\rho_s v_s) = 0 \quad (2)$$

Sum of volume fraction:

$$K_l + K_s = 1 \quad (3)$$

2.3.2 Momentum equation

Interaction between each phase is modeled by the force and interphase momentum each phase.

Fluid phase:

$$\rho_l k_l \left[\frac{\partial_v}{\partial_t} + v_l.\nabla v_l\right] = -k_l \nabla P + k_l \nabla \tau_l + \rho_l k_l g - M \quad (4)$$

Solid phase:

$$\rho_s k_s \left[\frac{\partial_v}{\partial_t} + v_s.\nabla v_s\right] = -k_s \nabla P + k_s \nabla \tau_s + \rho_s k_s g + M \quad (5)$$

$\frac{\partial}{\partial_t} = 0$ at steady state condition.

2.3.3 Closure model

A) Interphase Drag force model

Drag force per unit volume equation (spherical):

$$M_{d=\frac{3C_D}{4d_s}K_s\rho_l|v_s-v_l|(v_s-v_l)} \quad (6)$$

For solid volume fraction $K_s < 0.2$ or 20%, drag coefficient Wen and Yu model may used. This will assist ANSYS-CFX to apply appropiate limiting behaviour in intertial regimes as :

$$C_d = K_l^{-1.65}\max[\frac{24}{N'_{Rep}}\left(1+0.15N'^{0.687}_{Rep}\right),] \quad (7)$$

Where: $N'_{Rep} = K_l N_{Rep}\ and\ N_{Rep} = \rho_l \mid v_s - v_l \mid d_{s/M_l}$

While solid volume fraction greater than 20%, the Gidaspow drag model is use with the interphase drag force:

$$M_d = \frac{150(1-k_l)^2 M_l}{4d_s} + \frac{7}{4}\frac{(1-k_l)N_{Rep}}{M_l d_s} \quad K_s\rho_l \mid v_s - v_l \mid (v_s - v_l) \quad (8)$$

B) Lift force model

In two phase flow, force act perpendicularly to the motion called lift motion, while drag force in parallel to the flow. Two types of lift force employed by ANSYS are Mei lift and Saffman:

$$M_L = \frac{3}{2\Pi}\frac{\sqrt{u_t}}{d_s\sqrt{|\nabla X v_l|}}C'_L k_s\rho_l(v_s - v_l)X(\nabla X v_l + 2\Omega) \quad (9)$$

3.3 Geometry Modelling

Geometry of model generated using ANSYS 15.0 Workbench through CFX solver. Design modeler for geometry modeling is used to create a simple horizontal pipeline. Fully opened pipeline with 103mm diameter and 3500mm length is developed as shown in Table 1 below.

Table 1: Geometry modeling

Parameters	Values (mm)
Diameter	106
Length	3500

Diameter of pipe set to be 103mm based on [10], while length of pipe is calculated based on hydrodynamic calculation. Hydrodynamic was take into account as we were expecting a fully developed flow profile to be achieved beyond that length. As result we can concluded that length of the pipe is 44 times the pipe diameter (L=44D).

Hydrodynamic formula (turbulent):

$$L_h = 4.4\,(N_{RE})^{1/6}D$$

Where:

L_h : Hydrodynamic length

N_{RE} : Reynolds number

D : Diameter

3.4 Meshing and Grid Independence Study

Hexahedron meshing shape is utilized over other as for the same number of elements it is proved that hexahedron gives higher accuracy. While for grid independence study a graph relating pressure loss against element size is used (Figure 9).

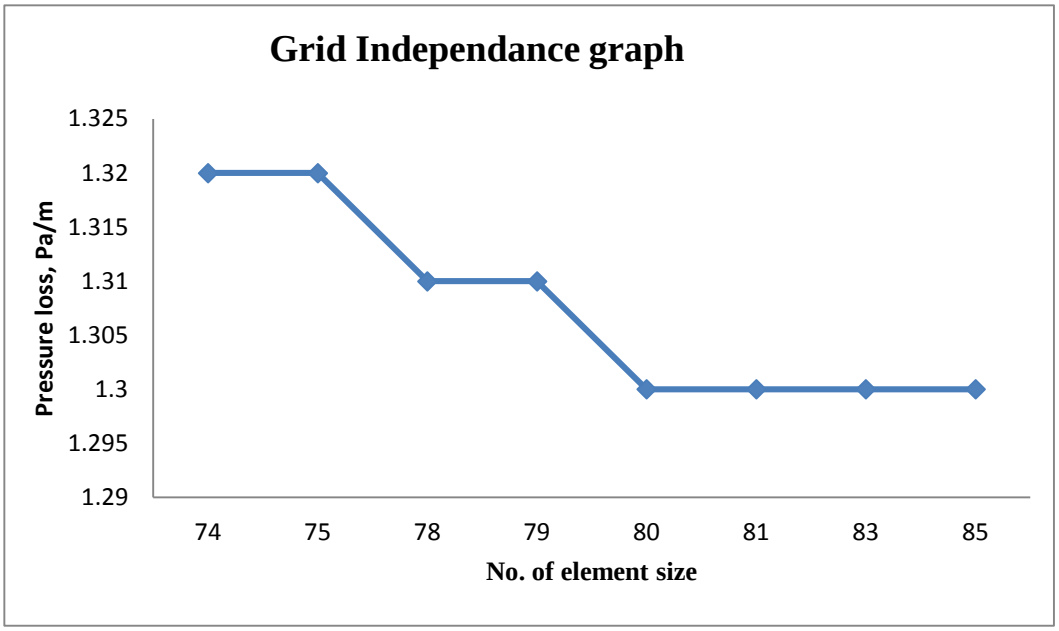

Figure 3: Pressure loss against Element size.

As we can see the trend started to reach a stable and consistence at element size of 80-85. In this study elements size of 82 is taken as optimum grid independence because it still can convey a good result as what 86 and above elements size able to deliver. On top of that simulation will takes lesser time to compute and produces results. Table 2 shows the selected meshing and grid independence information, while Figure 10 shows meshing 3-dimensional view.

Table 2 : Meshing and Grid Independence information

Parameters	Range
Meshing type	Hexahedron
Edge size (optimum)	82
No. of elements	801848
No. of nodes	840048

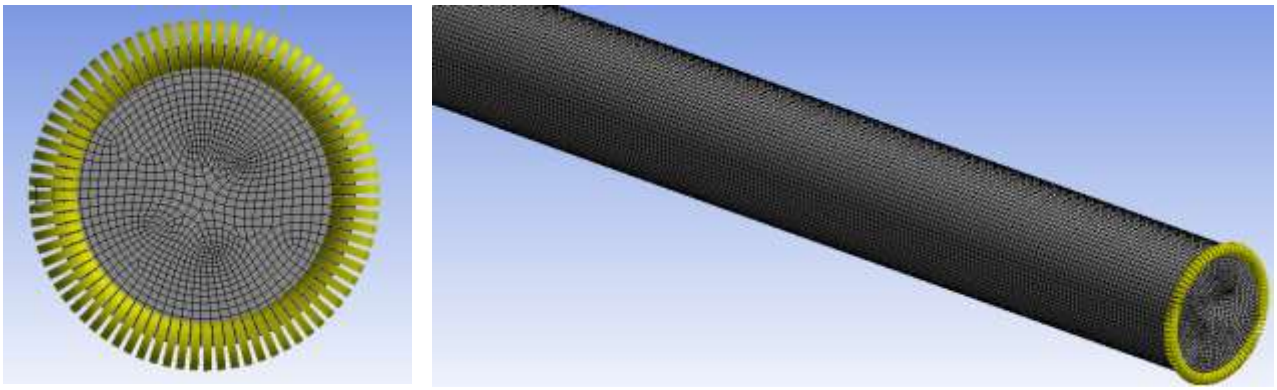

Figure 4 : Meshing 3-dimensional view

3.5 Boundary Condition

Boundary conditions are very important element in making simulation initialization model, without this it is impossible to have a satisfactory agreement between benchmark simulation models with experimental result.

In present work concentration and velocities at the inlet of both phases are specified, while in the outlet zero gauge pressure is specified. Average parabolic velocity profile and solids volume fraction are set as initial condition in order to initiate the numerical solution. At the wall liquid's velocities were set to non-slip condition (zero) for fluid phase, and free slip condition for solid phase were specified.

3.6 Parametric Study

Basically in this work, parametric study follows and experimental work done by [10], which will be validating after a simulation model is developed. Validated model will be use as benchmarking if an only if the performance is same with experimental study. Table 3 is the parametric done by [10].

3.7 Benchmarking: CFX Model Validation with Experimental Data

For this work, benchmark was inspired by the experimental case study carried by [10]. Before any parametric study can be done, the simulation has to be validate. After imitating all the experimental data needed, validation of simulation model becomes clearer by varying the turbulence equations. Below shows the experimental data done by [10] used as benchmarking validation table and also graphs showing the comparison between experimental result and simulation result.

Table 3 : Experimental Data by [10] used as Benchmarking Validation

Experimental Data	**Values**
Pipe Diameter	103mm
Pipe Length	3500mm
Size of particle	90-270 (μm)
Solid Volume Concentration	10-45 (%)
Specific Gravity of particle	2.65
Velocity of mixture	5.4 (m/s)
Turbulence Equation	-

As mentioned above the turbulence equation is varying in order to make validation of simulation become easier. There are many types of turbulence equation available in ANSYS but in this work only k-epsilon, k-Omega, SSG Reynold Stress, Shear Stress Transport, and Eddy Viscosity Transport were tested. Besides, Lifting force and Lubrication Force were not activated as is has no significant impact instead increase the time to completed the run.

3.7.1 The RNG k-epsilon model in ANSYS CFX

The RNG k-Ɛ model is based on Navier-Stokes equation which has been renormalize. The model constant is slightly differ where CƐ1 replaced by CƐ1RNG but transport equations for turbulence generation and dissipation are the same (standard k-Ɛ model). The transport for turbulence dissipation becomes:

$$\frac{\partial(\rho\varepsilon)}{\partial_t}+\frac{\partial}{\partial x_j}\left(\rho U_j\varepsilon\right)=\frac{\partial}{\partial x_j}\left[\left(\mu+\frac{\mu_t}{\sigma_{\varepsilon RNG}}\right)\frac{\partial\varepsilon}{\partial x_j}\right]+\frac{\varepsilon}{k}\left(C_{\varepsilon 1RNG}P_k-C_{\varepsilon RNG}\rho^{\varepsilon}+C_{\varepsilon 1RNG}P_{\varepsilon b}\right) \quad (10)$$

Where:

$$C_{\varepsilon 1\ RNG=1.42-f_\eta}$$

And

$$f_\eta=\frac{\eta\left(1-\frac{\eta}{4.38}\right)}{\left(1+\ \beta_{RNG}\eta^3\right)}$$

$$\eta=\sqrt{\frac{P_k}{\rho C_{\mu RNG}\in}}$$

3.7.2 The k-omega model

For k-omega equation Wilcox developed the initial point of present equation, it include two transport equation (kinetic energy, [k] and turbulence frequency, [ω]).

k-equation:

$$\frac{\partial(\rho k)}{\partial t}+\frac{\partial}{\partial_{xj}}\left(\rho U_j k\right)=\frac{\partial}{\partial_{xj}}\left[\left(\mu+\frac{\mu_t}{\sigma_k}\right)\frac{\partial_k}{\partial_{xj}}\right]+P_k-\beta'\rho k\omega+P_{kb} \quad (11)$$

ω-equation:

$$\frac{\partial(\rho\omega)}{\partial t}+\frac{\partial}{\partial_{xj}}\left(\rho U_j\omega\right)=\frac{\partial}{\partial_{xj}}\left[\left(\mu+\frac{\mu_t}{\sigma_\omega}\right)\frac{\partial_\omega}{\partial_{xj}}\right]+\propto\frac{\omega}{k}P_k-\beta\rho\omega^2+P_{\omega b} \qquad (12)$$

The model constant given by:

β'= 0.09 $\sigma_k = 2$

α = 5/9 $\sigma_\omega = 2$

β = 0.075

3.7.3 The SSG Reynold Stress

Reynolds Stress applicable when assumption of the eddy-viscosity no longer valid. The standard Reynolds Stress model in ANSYS-CFX is based on the ε-equation. The CFX-Solver utilize the following equations and solve for the transport of the Reynolds stresses:

$$\frac{\partial}{\partial x_k}\left(U_k\rho u_i u_j\right)=\frac{\partial}{\partial x_k}\left(\left(\mu+\frac{2}{3}C_s\rho\frac{k^2}{\varepsilon}\right)\frac{\partial u_i u_j}{\partial x_k}\right)+P_{ij}-\frac{2}{3}\delta_{ij}\rho\varepsilon+\phi_{ij} \quad (13)$$

Where ϕ_{ij} is pressure-strain correlation:

P_{ij} is the exact production term given by:

$$P_{ij}=-\overline{\rho u_i u_j}\ \frac{\partial U_j}{\partial X_k}\ -\overline{\rho u_j u_k}\ \ \frac{\partial U_i}{\partial X_k} \qquad (14)$$

As the turbulence dissipation arises in the stress equations individually, an equation for it is still required and takes the form:

$$\frac{\partial}{\partial X_k}(\rho U_k\varepsilon)=\frac{\varepsilon}{k}(C_{\varepsilon1}-C_{\varepsilon2}\rho\varepsilon)+\frac{\partial}{\partial X_k}[\left(\mu+\frac{\mu_t}{\sigma_{\varepsilon,RS}}\right)\frac{\partial\varepsilon}{\partial X_k}] \qquad (15)$$

The constants in the equations take the form:

$C_{\mu RS}=0.1, C_{\varepsilon RS}=1.36, C_{sl}=1.7, C_{s2}=-1.05, C_{rl}=0.9, C_{r2}=0.8,\ C_{r3}=0.65, C_{r4}=0.625, C_{r5}=0.2$

3.7.4 The Shear Stress Transport

The other turbulence model used in current study is The Shear Stress Transport where the k-ω based on (SST) model of Menter (1994). The transport equations for k and turbulence frequency (ω) are given by:

$$\nabla.(\rho Uk) = \nabla.\left[\left(\mu + \frac{\mu_t}{\sigma_{k3}}\right)\nabla k\right] + P_k - \beta^{'}\rho k\omega \quad (16)$$

$$\nabla.(\rho Uk) = \nabla.\left[\left(\mu + \frac{\mu_t}{\sigma_{\omega 3}}\right)\nabla \omega\right] + (1 - F_s)\rho\frac{2}{\sigma_{\omega 2}\omega}\nabla k\nabla\omega_{k} + \alpha_3\frac{\omega}{k}P_k - \beta_3\rho\omega^2 \quad (17)$$

The combined k-ε and k-ω models developed by not account for the transport of the turbulent shear stress consequently results in an over prediction of eddy-viscosity, and eventually bring to a wrong prediction of onset and the amount of flow separation from smooth surfaces. The proper transport behavior can be archived by a limiter to the formulation of the eddy-viscosity:

$$V_t = \frac{\alpha_l k}{\max(\alpha_l\omega, SF_2)};\ V_t = \frac{\mu_t}{\rho}$$

3.7.5 Eddy Viscosity Transport

Menter developed one simple equation which directly derived from k-ε model and is therefore named the (k-ε)1E model:

$$\frac{\partial\rho\tilde{\nu}_t}{\partial_t} + \frac{\partial\rho U_j\tilde{\nu}_t}{\partial_{xj}} = c_l\rho\tilde{\nu}_t S - c_2\rho(\frac{\tilde{\nu}_t}{\mathrm{L}_\nu K})^2 + [\left(\mu + \frac{\rho\tilde{\nu}_t}{\sigma}\right)\frac{\partial\tilde{\nu}}{\partial_{xj}}] \quad (18)$$

Where ν̃ is the kinematic eddy viscosity ν̃, and σ is a model constant. The model contains a destruction term which accounts for the turbulence of the structure. The model is based on the von Karman length scale:

$$(L_{\nu K})^2 = \left|\frac{S^2}{\frac{\partial S}{\partial_{xj}}\frac{\partial S}{\partial_{xj}}}\right|$$

Where S is the shear strain rate tensor. The eddy viscosity is computed from:

$$\mu_t = \rho \tilde{\nu}_t$$

In order to prevent a singularity of the formulation as the von Karman length scale goes to zero, the destruction term is reformulated as follows:

$$E_{k-\varepsilon} = (\frac{\tilde{\nu}_t}{L_{vK}})^2$$

$$E_{BB} = \frac{\partial \tilde{\nu}_t}{\partial_j} \frac{\partial \tilde{\nu}_t}{\partial_j} \quad (19)$$

$$E_{le} = c_3 E_{BB} \tanh(\frac{E_{k-\varepsilon}}{c_3 E_{BB}})$$

$$\frac{\partial \rho \tilde{\nu}_t}{\partial_t} + \frac{\partial \rho U_j \tilde{\nu}_t}{\partial_{xj}} = c_l D_l \rho \tilde{\nu}_t S - c_2 \rho E_{le} + [\left(\mu + \frac{\rho \tilde{\nu}_t}{\sigma}\right) \frac{\partial \tilde{\nu}_t}{\partial_{xj}}]$$

The coefficient are:

Coefficient	Value
C_1	0.144
C_2	1.86
C_3	7.0
A	13.5
K	0.41
σ	1.0

3.8 Design of Experiment

1. K-Ɛ turbulence model is chosen for the liquid phase.
2. Particles size varies from 90-270 µm.
3. Solid volume concentration varies from 10-40 %.
4. Mixture velocity is maintain at 5.4 m/s.

Table 4: Design of Experiment

Particle size. Dp (μm)	Solid conc. α s (%)	Mixture velocity (m/s)
90	10	5.4
	25	
	40	
150	10	
	25	
	40	
210	10	
	25	
	40	
270	10	
	25	
	40	

Table 5: Experimental parameters [10]

Parameter	**Values**
Fluid type	Water
Diameter of pipe	103mm
Size of particle	90-270 μm
Solid volume fraction	10-45%
Specific gravity of particle	2.65
Velocity of mixture	1.0-5.0 m/s

3.9 Key Milestone

Table 6: Key milestone

No	Milestone	Week
1	Literature Review	5
2	Modelling and Meshing geometry using ANSYS	9
3	Grid Independence Study	10
4	Benchmark problem (Model validation)	14
5	Studies the parametric and identify of all conditions (simulation)	19
6	Data collection and Result Analysis	26
7	Report and Technical Paper writing	28

3.9.1 Gantt Chart

Table 7: Gantt chart

	FYP1														FYP2											
Mission/Week (FYP)	1	2	3	4	5	6	7	8	9	10	11	12	13	14	15	16	17	18	19	20	21	22	23	24	25	26	27	28
Preliminary research objective and scope Determination																												
Identifying key point for benchmark problem																												
Model Validation of benchmark case study																												
Study the effect of particle size and solid pressure to slurry's behavior in pipeline																												
Studying the effect of types of flow to slurry's behavior in pipeline.																												
Data collection & results Analysis																												
Report Writing																												

CHAPTER 4
RESULT AND DISCUSSION

4.1 Benchmarking Study Result

Benchmarking study was conducted in order to validate the simulation model with the experimental. In other word, this is to ensure the model behaving or having the same performance as the real experiment. In this study, simulation model is set identically with the experimental parameters, condition and setup except turbulence equation. The validation judgement is done by varying the turbulence equation.

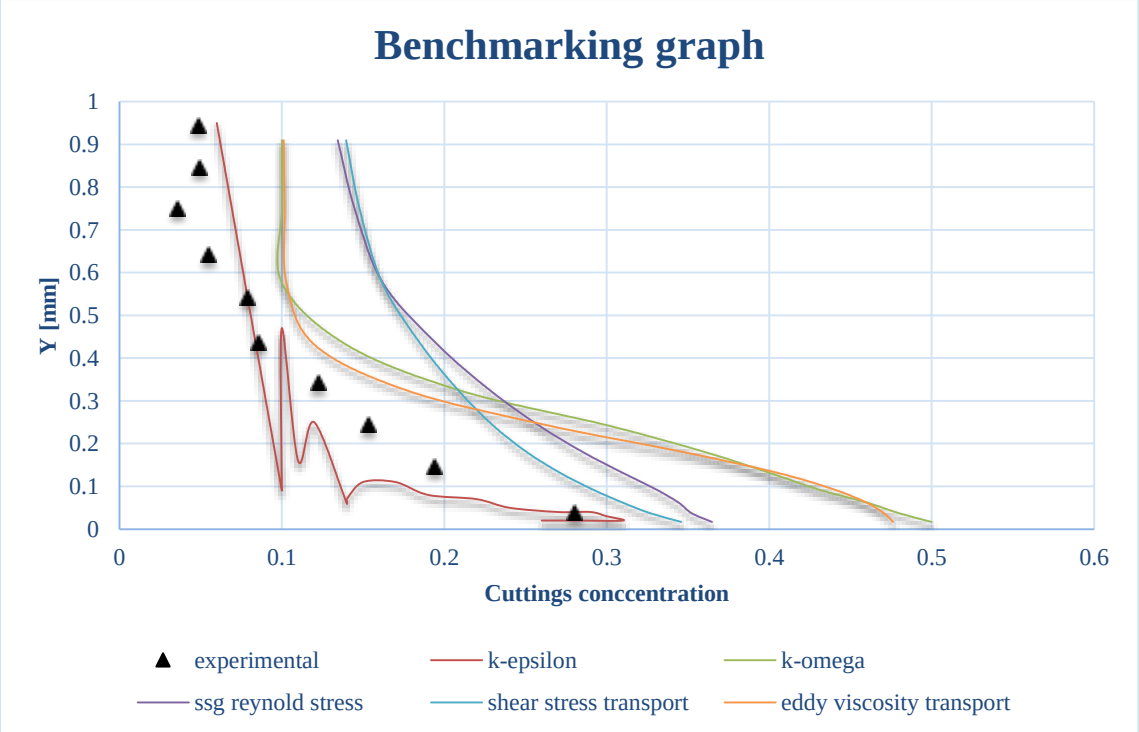

Figure 5: Benchmarking Graph

From Figure 11, clearly shown that by taking k-Epsilon as Simulation turbulence equation it gives the closes curve to the Experimental Result, meaning this study agrees with [4,7]. Therefore in this study, benchmarking study is said to be archived by taking k-Epsilon as turbulence equation.

4.2 Cutting Volume Fraction

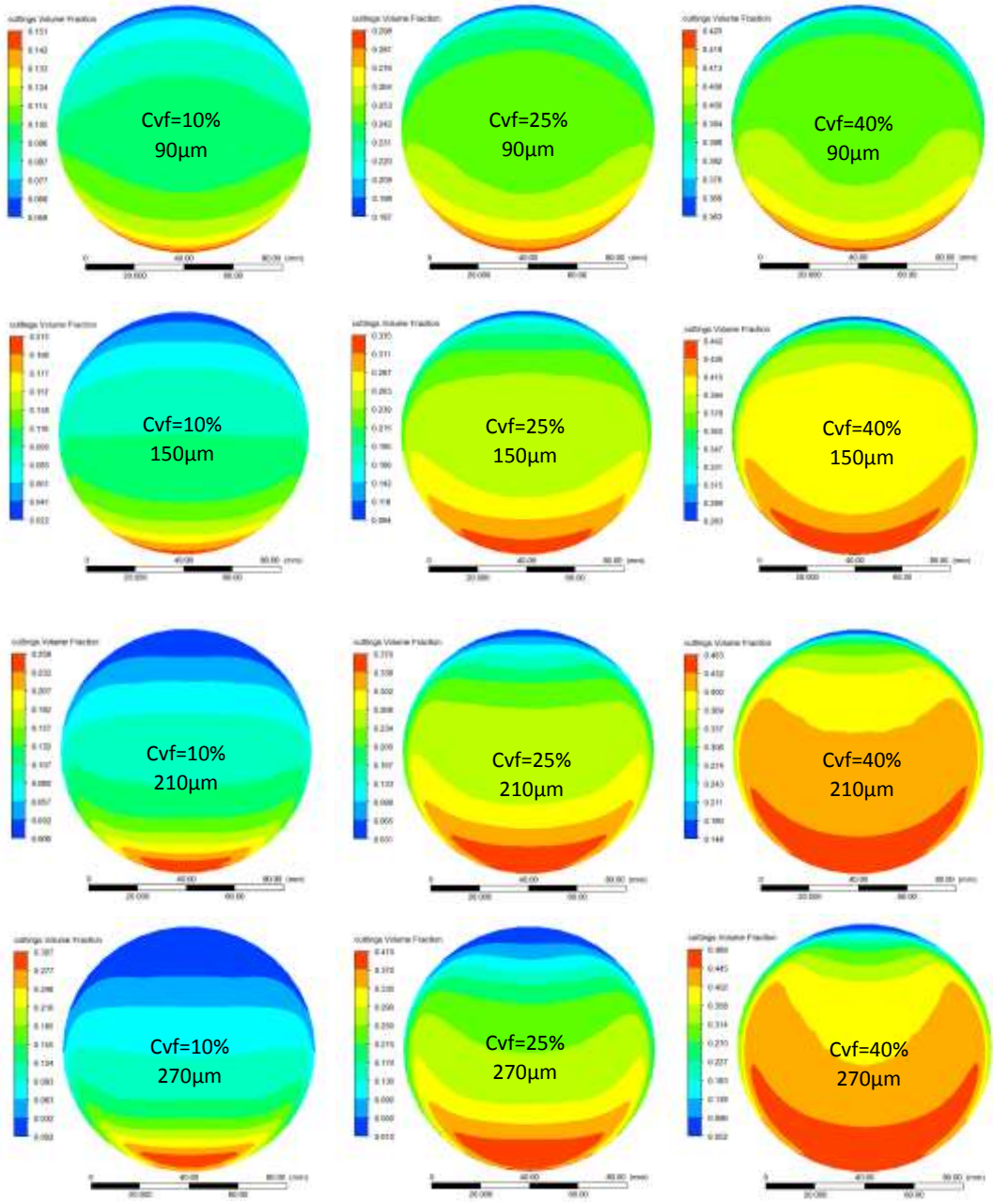

Figure 6: Cutting concentration at outlet with variation particle sizes and cutting volume fraction at mixture's velocity of 5.4 m/s

Figure 6 and 15 (appendix) showing cutting concentration at outlet with variation particle sizes and cutting volume fraction at mixture's velocity of 5.4 m/s. from left to right 2D diagram showing increasing in cutting volume fraction from 10, 25 and 40%. Result in simulation showing that cutting concentration (at outlet) increased as increasing the cutting volume fraction injected into the system (pipe) at all

particle size. This is because cutting volume fraction injected is directly proportional to the amount of solid enters the system, the higher the volume fraction the higher amount of solid particle in pipe. Therefore 40% of cutting volume fraction having the highest cutting concentration (in the outlet) at all particle size distribution. While going down showing increasing in particle size from 90, 150, 210 and 270μm. Size of particle influence particle propensity to deposit at bottom of pipe due to gravity. The bigger the particle the heavier it be, thus more likely to be pulled by gravity. Therefore in this simulation cutting with bigger size will have more visible result in term of cutting concentration compared to small particle size at all volume fraction.

4.3 Effect of Particle Size on Pressure Loss at Various Cutting Volume Fraction

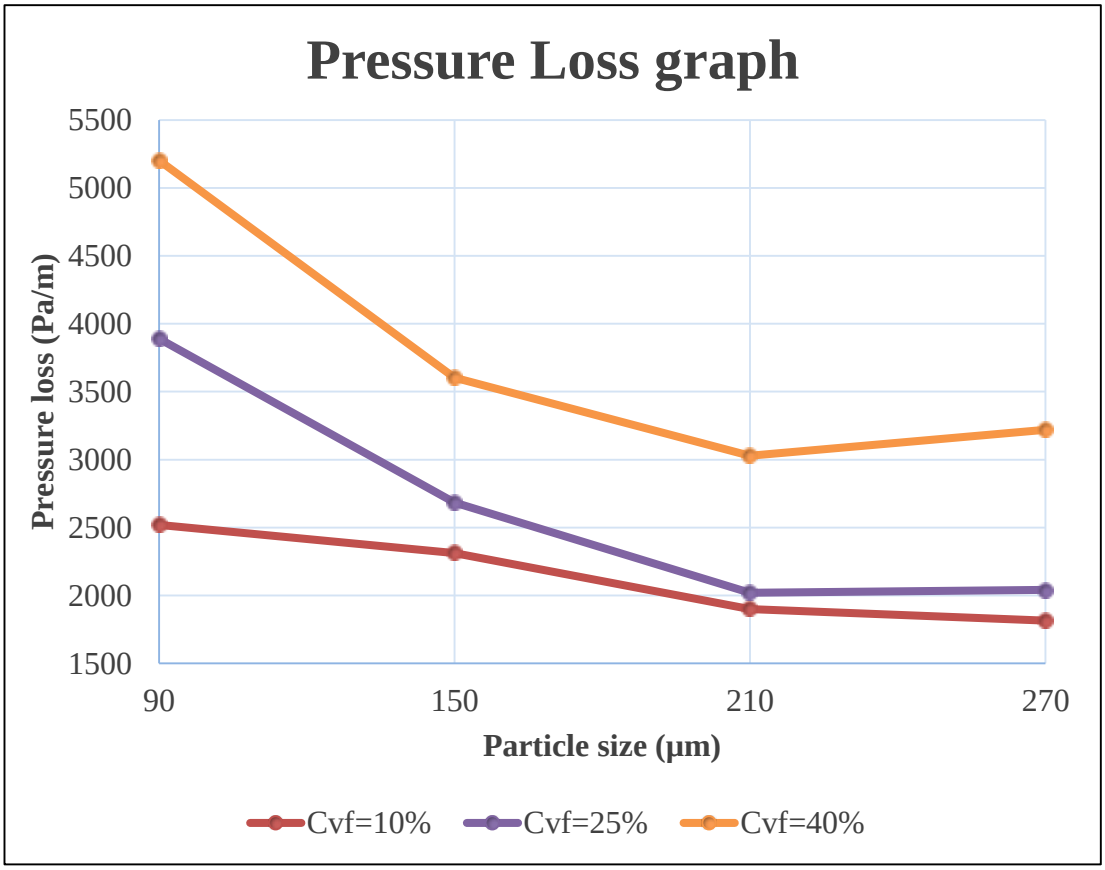

Figure 7: Effect of Particle size on Pressure loss at various cutting volume fraction.

From Figure 7, the CFD predicted that higher cutting concentration have higher pressure loss. This is because particle try to settling radially due to gravity forces which consequently create friction to carrier fluid moving in axial direction.

Increasing more cutting fraction creates more resistance and therefore higher pressure loss plotted. On the other hand, presence of particle in the flow of carrier fluid introduces three additional friction sources to the system, there are particle to particle, fluid to particle and particle to wall friction. The CFD predicted the higher the particle size the smaller the pressure loss which is contradicting to [10] as he found "finer particles prone to have less pressure loss (at all concentration and velocities) than medium and coarser particles". This is due to as particle size increases the smaller the total effective flow area (as can be seen in Figure 6 and 7), thus increase in effective flow velocity. Higher the velocity will decrease the friction as friction is indirectly proportional to the Reynold number. Therefore the lesser the friction the lower pressure loss as there are indirectly proportional to each other.

However this result become more interesting as there are changing in the pressure loss trend line at higher cutting volume fraction (25% and 40%) for particle size of 270µm. What influenced the sudden increment in pressure loss are at 270µm the particle is relatively big to the diameter of the pipe used in this study therefore the deposited particle not only reduced the effective flow area it also starts to block the pipe. Besides higher volume fraction of cutting is injected into the system increase the amount of particle entered the system, cuttings not only deposited but they also moving along with the carrier fluid which consequently increase the friction in the pipe. Therefore increment of pressure loss plotted at particle size of 270µm at high cutting volume fraction.

4.4 Effect of Particle Size on Radial Particle Concentration Profile

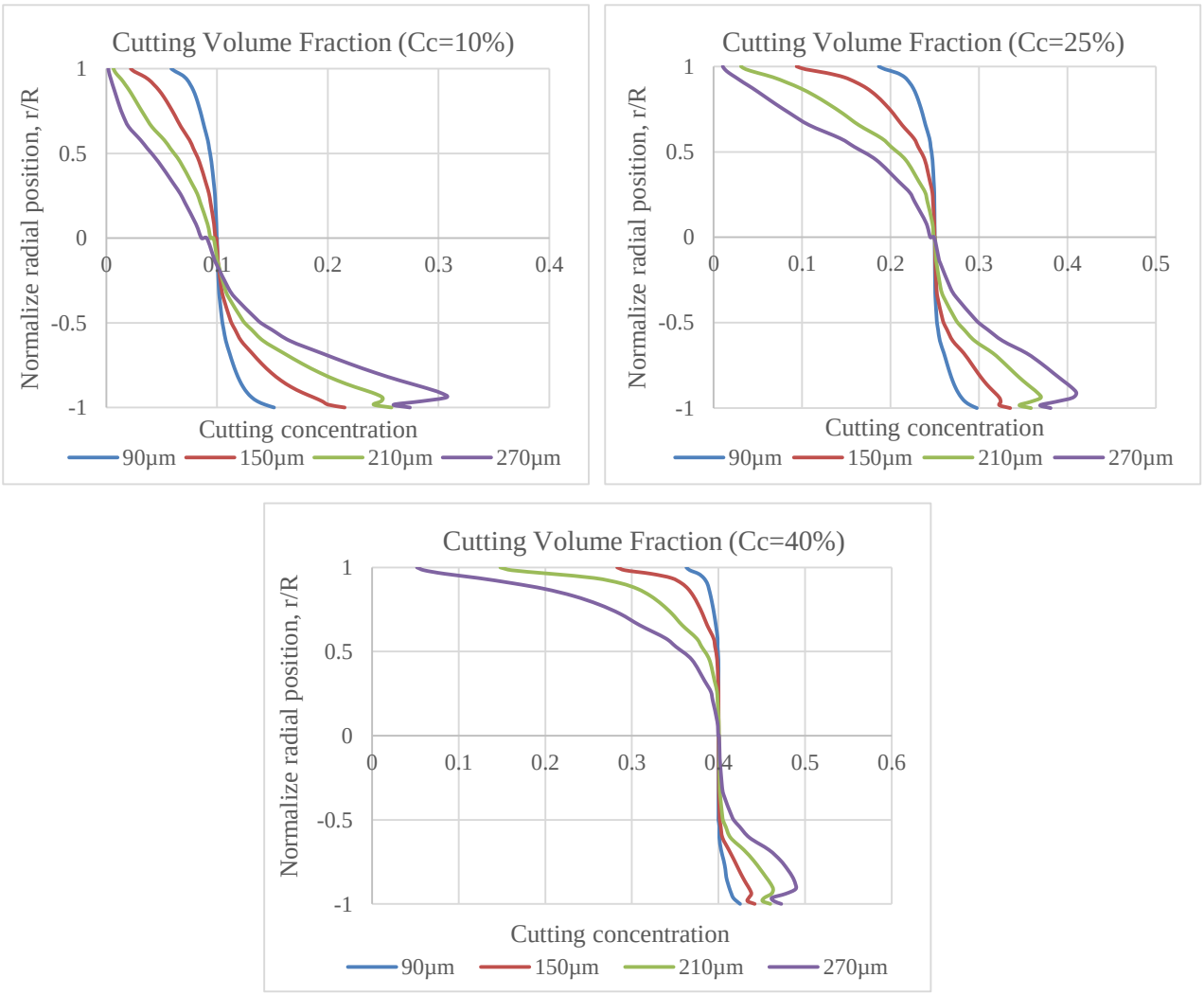

Figure 8: Effect of Particle size on Radial particle concentration profile at different cuttings volume fraction (10%, 25% and 40%).

Figure 8 showing the effect of particle size on radial particle concentration profile at the various cutting volume fraction (10%, 25% and 40%). Generally there are three areas can be identified. First, low concentration area close to the top of pipe. Second, central area where the concentration found almost at similar at initial cutting concentration. Last, is the area where high concentration settles at bottom of the pipe with the cutting volume fraction that greater than mean value. Particle settling becomes more remarkable as the particle diameter increased, leading to higher concentrations area (approaching) at bottom of pipe. Compared to bigger particle size, the small form a uniform radial distribution as smaller particle naturally in buoyant.

4.5 Effect of particle size and volume fraction on cuttings velocity

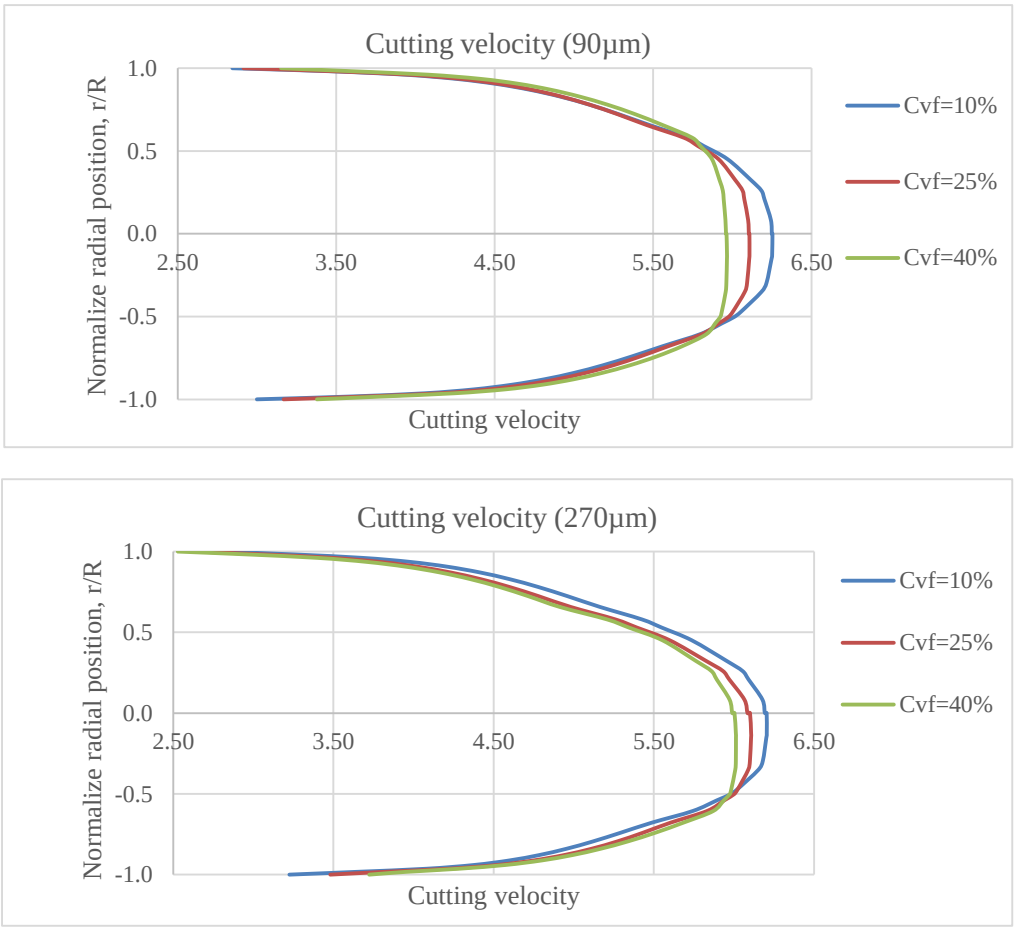

Figure 9: Effect of particle size and cutting volume fraction on cutting velocity

Figure 9 shows the effect of particle size on cutting velocity. Sample result are only obtained from particle size of 90µm and 270µm as both having more visible in comparison. Generally, from both result cutting velocity profile behaving asymmetrical about the central axis, but from here it is shown that degree of asymmetry is influenced by particle size which rhymes with what [17] had found. At particle size of 270µm cutting velocity plot skewed to the bottom of the pipe, this is result of particle settling due to difference mass of two different particle size. On the other hand, both particle size agrees that small cutting volume fraction leads to fastest cutting velocity followed by medium and large cutting volume fraction.

CHAPTER 5
CONCLUSION AND RECOMMENDATIONS

Simulation result shows reasonably good agreement with the published experimental data. The profile pattern in those results matches the theoretical knowledge understanding by taking K-Epsilon model as turbulence equation. To conclude Computational Fluid Dynamic (CFD) has a credibility to validate the behavior of slurry flow in pipeline.

The CFD simulation model was then used to study the cutting concentration at outlet with variation particle sizes and cutting volume fraction (at mixture's velocity of 5.4 m/s), which resulting cuttings tend to accumulate at the end of the pipe as particles lose their momentum due to gravity.

Increasing the cutting volume fraction resulting increase the pressure loss in the simulation outcome, but larger particle sizes results in lower pressure loss due to lower friction between particle and particle, particle to fluid and particle to wall.

Finally, particle settling becomes more pronounced for larger particle sizes, leading to higher particle concentrations near the bottom of the pipe.

As a recommendation running simulation relating two phase between solid and liquid should consider K-Epsilon as turbulence equation. Second, since cuttings tend to accumulate at end of pipe due to gravity therefore lighter and smaller particle should be used especially in long-range pipeline. Third, lower the cutting volume fraction in order to have smaller pressure losses which will increase the efficiency of cementing or hydraulic fracturing operation. Finally, since particle settling becomes more remarkable as the particle diameter increased thus leading to higher concentrations area (approaching) at bottom of pipe. Therefore, finer particle size should be employ in transporting slurry in pipeline.

REFERENCES

[1] Chong Y, W. C. (February 2014). CFD Modelling and Experimental Observation of Changing Surface Profiles Caused by Solid-Particle Erosion. SPE Production & Operation.

[2] Ghanta, S. K. (2010). Slurry Flow Modelling By CFD. CI & CEQ.

[3] Kalekudhiti Ekambara, R. S. (2009). Hydrodynamic Simulation of Horizontal Slurry Pipeline Flow Using ANSYS-CFX.

[4] Lahiri, S. (December 2008). Computational Fluid Dynamic Simulation of the Solid Liquid Slurry Flow in a Pipeline. SELECTED WORK.

[5] Titus N. Ofei, Sonny Irawan, and William Pao. (April 2014). CFD Method for Predicting Annular Pressure Losses and Cuttings Concentration in Eccentric Horizontal Wells.

[6] R.Rosine, M. B. (2005). Fluid-Flow Phenomena in CT Using CFD. SPE 94057.

[7] Tamer Nabil, Imam El-Sawaf and Kamal El-Nahhas. (March 2014). SAND WATER SLURRY FLOW MODELLING IN A HORIZONTAL PIPELINE BY COMPUTATIONAL FLUID DYNAMICS TECHNIQUE. International Water Technology Journal, IWTC.

[8] Roco, M. C.; Shook, C. A. Modeling of Slurry Flow: The Effect of Particle Size. Can. J. Chem. Eng. 1983, 61, 494–503.

[9] Roco, M. C.; Mahadevan, S. Modeling Slurry Flow, Part 1, Turbulent Modeling. J. Energy Res. Technol. 1986, 108, 269–277.

[10] Gillies, R. G.; Shook, C. A.; Wilson, K. C. An Improved Two- layer Model for Horizontal Slurry Pipeline Flow. Can. J. Chem. Eng. 1991, 69, 173–178.

[11] Hunt, J. N. The Turbulent Transport of Suspended Sediment in Open Channels. R. Soc. London, Proc., Ser. A 1954, 224, 322–335.

[12] Karabelas, A. J. Vertical Distribution of Dilute Suspensions in Turbulent Pipe Flow. AIChE J. 1977, 23, 426–434.

[13] Kaushal, D. R.; Tomita, Y.; Dighade, R. R. Concentration at the Pipe Bottom at Deposition Velocity for Transportation of Commercial Slurries through Pipeline. Powder Technol 2002, 125, 89–101.

[14] Kaushal, D. R.; Tomita, Y. Comparative Study of Pressure Drop in Multisized Particulate Slurry Flow through Pipe and Rectangular Duct. Int. J. Multiphase Flow 2003, 29, 1473–1487.

[15] Kaushal, D. R.; Sato, K.; Toyota, T.; Funatsu, K.; Tomita, Y. Effect of Particle Size Distribution on Pressure Drop and Concentration Profile in Pipeline Flow of Highly Concentrated Slurry. Int. J. Multiphase Flow 2005, 31, 809–823.

[16] Seshadri, V.; Singh, S. N.; Kaushal, D. R. A Model for the Prediction of Concentration and Particle Size Distribution for the Flow of Multisized Particulate Suspensions through Closed Ducts and Open Chan- nels. Part. Sci. Technol 2006, 24, 239–258.

[17] Kaushal, D. R.; Tomita, Y. Experimental Investigation of Near- Wall Lift of Coarser Particles in Slurry Pipeline Using Gamma-ray Densitometer. Powder Technol 2007, 172, 177–187.

[18] Walton, I. C. Eddy Diffusivity of Solid Particles in a Turbulent Liquid Flow in a Horizontal Pipe. AIChE J. 1995, 41, 1815–1820.

[19] Wasp, E. J., Kenny, J. P., Gandhi, R. L. Solid Liquid Flow Slurry Pipeline Transportation, 1st ed.; Trans. Tech. Publications: Clausthal, Germany, 1977.

[20] Wilson, K. C. A Unified Physical-based Analysis of Solid-Liquid Pipeline Flow. Proceedings of the 4th International Conference of Hydraulic Transport of Solids in pipes (Hydrotransport 4), BHRA Fluid Engineering: Cranfield, U.K., Paper A1, 1976; 1-16.

[21] Doron, P.; Granica, D.; Barnea, D. Slurry Flow in Horizontal Pipes-Experimental and Modeling. Int. J. Multiphase Flow 1987, 13, 535–547. (8) Wilson K. C.; Pugh, F. J. Dispersive-Force Modeling of Turbulent Suspension in Heterogeneous Slurry Flow. Can. J. Chem. Eng. 1988, 66, 721– 727.

[22] Nassehi, V.; Khan, A. R. A Numerical Method for the Determination of Slip Characteristics between the Layers of a Two-Layer Slurry Flow. Int. J. Numer. Method Fluids 1992, 14, 167–173.

[23] Doron, P.; Barnea, D. A Three-Layer Model for Solid-Liquid Flow in Horizontal Pipes. Int. J. Multiphase Flow 1993, 19, 1029–1043.

[24] Ramadan, A.; Shalle, P.; Saasen, A. Application of a Three-Layer Modeling Approach for Solids Transport in Horizontal and Inclined Channels. Chem. Eng. Sci. 2005, 60, 2557–2570.

APPENDIXES

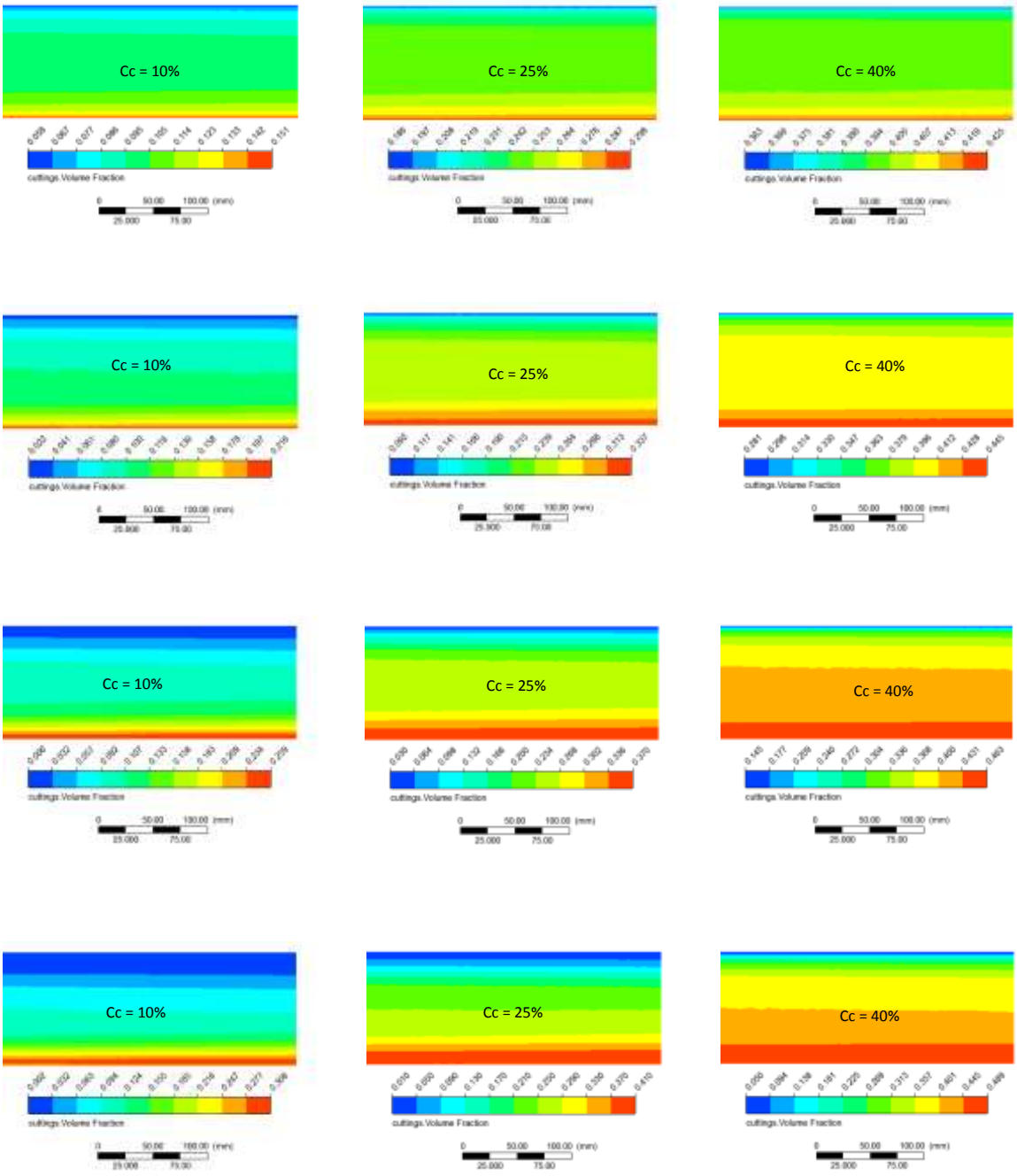

Figure 10: Cutting volume fraction at outlet with variation particle sizes and cutting concentration at mixture's velocity of 5.4 m/s (side view)

Nomenclature and symbol

C_{R1}	Linear resistance coefficient	r	Shear stress
C_{R2}	Quadratic resistance coefficient	u	Fluctuating velocity component in turbulent flow
$C_{\varepsilon 1}$	k-Ɛ turbulence model constant (1.44)	Ɛ	Turbulent dissipation rate
$C_{\varepsilon 1\ RNG}$	RNG k-Ɛ turbulence model coefficient (1.42-f_h)	$O_{\varepsilon}RS$	Reynold stress model constant
$C_{\varepsilon 2}$	k-Ɛ turbulence model constant (1.92)	$O_{k}RNG$	RNG k-Ɛ turbulence model constant (0.7179)
$C_{\varepsilon 1\ RNG}$	RNG k-Ɛ turbulence model coefficient (1.68)	$O_{\varepsilon}RNG$	RNG k-Ɛ turbulence model constant (0.7179)
C_{μ}	k-Ɛ turbulence model constant (0.09)	ν	Specific volume
$C_{\mu\ RS}$	Reynold Stress model constant	ϕ	Additional variable (non-reacting scalar)
$C_{\mu\ RNG}$	RNG k-Ɛ turbulence model constant (0.085)	β	coefficient of thermal expansion (for the Boussinesq approximation)
ID	Internal diameter	β_{RNG}	RNG k-Ɛ turbulence model constant (0.012)
N_{Rep}	Reynold Number	ρ	density
$\mathcal{M}_g$	Fluid viscosity	K_s	Volume fraction solid
L_h	Hydrodynamic length	K_l	Volume fraction liquid
D	Diameter	C_d	Drag coefficient
μ	Viscosity	d_s	Diameter particles
$\boldsymbol{U}$	Vector of velocity $U_{x,y,z}$	ϕ_{ij}	Pressure strain correlation
U	Velocity magnitude		